Post-print version of the following article published in Reproduction Fertility and Development

In vitro maturation affects chromosome segregation, spindle morphology and acetylation of lysine 16 on histone H4 in horse oocytes

Federica Franciosi[A,I], Ghylene Goudet[B,C,D,E], Irene Tessaro[A], Pascal Papillier[B,C,D,E], Rozenn Dalbies-Tran[B,C,D,E], Fabrice Reigner[F], Stefan Deleuze[G], Cecile Douet[B,C,D,E], Ileana Miclea[H], Valentina Lodde[A] and Alberto M. Luciano[A]

[A]Reproductive and Developmental Biology Laboratory, Department of Health, Animal Science and Food Safety, University of Milan, via Celoria, 10, Milan, 20133, Italy.

[B]INRA, UMR85 Physiologie de la Reproduction et des Comportements, Nouzilly, F-37380, France.

[C]CNRS, UMR7247, Nouzilly, F-37380, France.

[D]Universite´ Franc¸ois Rabelais, 60 Rue du Plat d'Etain, Tours, F-37000, France.

[E]IFCE, Nouzilly, F-37380, France.

[F]INRA, UEPAO, Nouzilly, F-37380, France.

[G]Universite´ de Liège, Clinique des Animaux de Compagnie et des Equidés, Place du 20 Aout 7, Liège, 4000, Belgium.

[H]University of Agricultural Sciences and Veterinary Medicine, Calea Manatur 3-5, Cluj-Napoca 400372, Romania.

[I]Corresponding author. Email: federica.franciosi1@unimi.it

***Reproduction Fertility and Development*, Volume 29, Issue 4, April 2017, Pages 721–730, doi: 10.1071/RD15350**

Received: 28 August 2015; Accepted: 12 November 2015; Published online: 14 December 2015

Link to publisher site: https://www.publish.csiro.au/RD/RD15350

Abstract

Implantation failure and genetic developmental disabilities in mammals are caused by errors in chromosome segregation originating mainly in the oocyte during meiosis I. Some conditions, like maternal ageing or in vitro maturation (IVM), increase the incidence of oocyte aneuploidy. Here oocytes from adult mares were used to investigate oocyte maturation in a monovulatory species. Experiments were conducted to compare: (1) the incidence of aneuploidy, (2) the morphology of the spindle, (3) the acetylation of lysine 16 on histone H4 (H4K16) and (4) the relative amount of histone acetyltransferase 1 (HAT1), K(lysine) acetyltransferase 8 (KAT8, also known as MYST1), histone deacetylase 1 (HDAC1) and NAD-dependent protein deacetylase sirtuin 1 (SIRT1) mRNA in metaphase II stage oocytes that were in vitro matured or collected from peri-ovulatory follicles. The frequency of aneuploidy and anomalies in spindle morphology was increased following IVM, along with a decrease in H4K16 acetylation that was in agreement with our previous observations. However, differences in the amount of the transcripts investigated were not detected.

These results suggest that the degradation of transcripts encoding for histone deacetylases and acetyltransferases is not involved in the changes of H4K16 acetylation observed following IVM, while translational or post-translational mechanisms might have a role. Our study also suggests that epigenetic instabilities introduced by IVM may affect the oocyte and embryo genetic stability.

Additional keywords: aneuploidy, histone acetyl-transferases, histone deacetylases, meiosis

Introduction

Implantation failure, miscarriages and genetic developmental disabilities in mammals are often caused by errors in chromosome segregation that result in aneuploidy. Most of these errors originate in the oocyte during meiosis I (Hassold and Hunt 2001). Despite efforts to unravel the underlying molecular basis of chromosomal mis-segregation, a defined mechanism has not been identified. Several genetic, epigenetic and biochemical mechanisms have been proposed from different research groups, including defective spindle assembly checkpoint (Jones and Lane 2013; Yun et al. 2014), weakened centromere cohesion (Chiang et al. 2010; Eichenlaub-Ritter 2012; Tsutsumi et al. 2014), alterations in the pattern of histone covalent modifications (Akiyama et al. 2006; Yang et al. 2012; Luo et al. 2013; Ma and Schultz 2013), altered microtubule–kinetochore interactions (Shomper et al. 2014), sites and level of recombination (Cheng et al. 2009; Shin et al. 2010; Li et al. 2011), cell cycle regulation defects (Homer et al. 2005; Nabti et al. 2014) and mitochondrial dysfunction (Bartmann et al. 2004; Eichenlaub-Ritter et al. 2004). While this intricate scenario likely indicates that the origin of aneuploidy is multifactorial and aneuploidies arise from different mechanisms, some conditions in the mother, such as age (te Velde and Pearson 2002) or obesity (Luzzo et al. 2012), are known to increase the occurrence of chromosomal mis-segregation. Moreover, a higher incidence of aneuploidy has also been described following in vitro maturation (IVM; Nogueira et al. 2000; Emery et al. 2005; Roberts et al. 2005; Nichols et al. 2010), indicating that events that take place in a short time period (hours) can be sufficient to induce errors in chromosome segregation.

Using an adult, naturally cycling, monovulatory animal model (the horse), we recently observed that in oocytes that were in vitro matured the global acetylation pattern of histone H4 at the residue lysine (K) 16 was altered following IVM compared with in vivo-matured oocytes. Remarkably, other H4 N-terminal K residues such as K8 and K12 were not affected (Franciosi et al. 2012). In the present study we investigated whether, in the same animal model, IVM can also affect the ability to form a regular spindle and normal chromosome segregation. Global acetylation at H4K16 is thought to be one of the key epigenetic regulators in somatic and germ cells, especially for chromatin remodelling and chromosome condensation (Ma and Schultz 2013). Therefore, even though its function during meiosis is not clear, it is likely that the alteration of H4K16 acetylation affects chromosomal alignment during meiosis I.

In somatic cells histone acetylation is generally associated with active gene transcription (as reviewed in Clayton et al. 2006; Turner 2014; Zentner and Henikoff 2014). However, a transcriptionally inactive state is established during the last phase of oocyte growth and maturation. The regulation of gene expression at this time, and until the embryonic genome is activated, relies on post-transcriptional events of previously stored maternal mRNAs (Chen et al. 2011). One of the described post-transcriptional regulatory mechanisms consists in the selective degradation of specific maternal mRNAs (Chen et al. 2011; Ma et al. 2013).

The interplay between several classes of histone deacetylases (HDACs) and histone acetyltransferases (HATs) is responsible for acetylation at specific histone residues (Lombardi et al. 2011; Marmorstein and Zhou 2014). Therefore, in the present study we investigated the total mRNA amount of four histone

acetylation-related enzymes – HAT1, K(lysine) acetyltransferase 8 (KAT8, also known as MYST1), HDAC1 and NADdependent protein deacetylase sirtuin 1 (SIRT1) – in horse oocytes that were matured in vivo or in vitro. With this study we started to investigate the molecular mechanism that might interfere with the acetylation state of H4K16 during IVM.
Compared with rodent animal models, the horse does not allow genetic manipulations, is less easy to manipulate and its maintenance is more expensive. However, because of the similarity in the ovarian follicular waves and ovulation of one dominant follicle to human ovarian physiology, the horse model is gaining considerable interest for the study of oocyte maturation (Ginther et al. 2004; Carnevale 2008; Donadeu and Pedersen 2008; Ginther 2012), oocyte quality (Cox et al. 2015) and as a model of reproductive aging (Campos-Chillon et al. 2015; Hendriks et al. 2015; Ruggeri et al. 2015).

Materials and methods

All the procedures were approved by the Animal Care and Use Committee CEEA Val de Loire Number 19 and performed in accordance with the Guiding Principles for the Care and Use of Laboratory Animals.
All chemicals were purchased from Sigma-Aldrich (St. Quentin Fallavier, France or Milan, Italy) unless otherwise indicated.

Oocyte collection and in vitro maturation

Oocytes were collected by transvaginal ultrasound-guided aspiration from 32 adult cyclic pony mares (3–12 years old) housed at the facilities of INRA, Nouzilly. Based on mare reproductive physiology, standard breeding and veterinary practice and previous studies (Carnevale 2008; Rambags et al. 2014; Campos-Chillon et al. 2015; Ruggeri et al. 2015) mares 3–12 years old were used because they are considered to be young but already mature in terms of reproductive performance. Collection procedures were conducted as previously described (Luciano et al. 2006; Franciosi et al. 2012). Briefly, the ovaries were daily assessed by ultrasound scanning and at the emergence of a follicle >33mm the mares were injected i.v. with 1500 IU human chorionic gonadotrophin (hCG; Chorulon; Intervet, Beaucouze´, France). The in vivo-matured oocytes (one per mare) were collected by transvaginal ultrasound-guided aspiration of the pre-ovulatory follicle 35 h after hCG injection. Only oocytes with a well-extruded polar body (28/32: 88% maturation rate) were considered to be mature and further used in downstream procedures (16 for immunofluorescence and 12 for reverse transcription quantitative polymerase chain reaction (RT-qPCR), respectively); the others were discarded.
Fifty-eight germinal vesicle (GV)-stage oocytes were collected from follicles 5 and 25mm in diameter. Attempts to retrieve GV-stage oocytes from follicles >33mm of mares not treated with hCG were not successful because of the limited number of follicles at this stage of development. Fourteen of those collected were used for mRNA extraction, while the remaining 44 were matured in vitro as previously described (Franciosi et al. 2012) and used in downstream procedure (25 for immunofluorescence and 12 for RT-qPCR, respectively). Briefly, IVM procedures consisted of culture in TCM199 supplemented with 20% fetal calf serum (FCS; Gibco by Life Technologies, Carlsbad, CA, USA), 0.68mM L-glutamine, 25mM NaHCO3, 0.2mM sodium pyruvate and 50 ng/mL epidermal

growth factor in humidified air with 5% CO2 at 38.5°C for 28 h. Only oocytes that after 28 h IVM showed a well-extruded polar body (37/44: 85% maturation rate) were considered to be mature and further used in downstream procedures; the others were discarded.

Chromosome count

Chromosome-counting procedures were adapted from Duncan et al. (2009) and Chiang et al. (2010). After 28 h IVM or after collection from the pre-ovulatory follicle, the cumulus-enclosed oocytes were cultured for 1 h in the presence of 100 mM monastrol. The cumulus cells were then removed by treatment in 0.5% hyaluronidase or by gentle pipetting and the zona pellucida was digested in 0.2% pronase. The oocytes were fixed in 4% paraformaldehyde in phosphate-buffered saline (PBS) for 15 min at 38.58C followed by a further 45 min at 48C, extensively washed in PBS–polyvinyl alcohol (PVA) and permeabilised in 0.3% Triton X-100 for 10 min at room temperature. Non-specific binding was blocked by incubation in PBS with 1% bovine serum albumin (BSA) and 10% normal donkey serum for 30 min at room temperature. Oocytes were then incubated in a solution of rabbit anti-Aurora B phospho-Thr232 (636102; Biolegend, San Diego, CA, USA) in PBS with 1% BSA (dilution 1 : 50) at 48C overnight. After extensive washing, the oocytes were incubated in a solution of tetramethylrhodamine isothiocyanate (TRITC)-conjugated donkey anti-rabbit IgG (1 : 100 in PBS with 1% BSA) for 1 h at room temperature in the dark, then washed again and mounted on slides in the anti-fade medium VectaShield (Vector Laboratories Inc., Burlingame, CA, USA) supplemented with 20 mM YOPRO1 (Invitrogen by Life Technologies).

The samples were analysed on a laser-scanning confocal microscope (LSM 780; Zeiss, Oberkochen, Germany). Images were taken spanning the whole metaphasic plate on the z-axis every 0.35 μm. The chromosome number was counted in serial confocal sections by using NIH ImageJ 1.4 Software (rsb.info. nih.gov/ij/download.html). Specifically, the serial sections are piled, but only one layer is visualised at a time. By going back and forth from one section to the other, chromosomes that appear, stay and disappear in sequential sections are identified with a numeric code. The centromere marker, by staining a much smaller volume compared with the chromosome volume, allows tracking of the overlapping chromosomes that are otherwise hardly distinguishable on the 2D reconstructed image.

The staining of the centromeric region with the Aurora B phospho-(Thr232) was used to identify different chromosomes on sequential plans. The chromosomal count was carried out blindly by two independent operators and expressed as 32 (euploid), >32 (hyperploid) or <32 (hypoploid).

Spindle and acH4K16 immunostaining

Immunostaining procedures were adapted from Goudet et al. (1997). Cumulus cells were removed by treatment in 0.5% hyaluronidase or by gentle pipetting, briefly washed in Dulbecco's PBS with 0.1% PVA and fixed in 2.5% paraformaldehyde for 20 min at 388C. The oocytes were then washed, permeabilised in 0.1% Triton X-100 for 5 min at room temperature and non-specific binding was blocked by incubation with 10% normal donkey serum, 2% BSA and 0.05% saponin for 2 h at room temperature. The oocytes were

incubated overnight at 48C in a solution of mouse anti-a-tubulin (1 : 150) and rabbit anti-acH4K16 (1 : 250; Upstate Biotechnology Inc., Lake Placid, NY, USA) in PBS with 2% BSA and 0.05% saponin.
After extensive washing, the oocytes were incubated in a solution of AlexaFluor 488-coniugated donkey anti-mouse IgG (1 : 500; Invitrogen byLife Technologies) andTRITC-conjugated donkey anti-rabbit IgG (1 : 100; Vector Laboratories Inc.) in PBS with 2% BSA and 0.05% saponin for 1 h at room temperature in the dark. After extensive washing, the samples were mounted on slides in VectaShield supplemented with 1 mg/mL 40,6-diamidino-2-phenylindole (DAPI).
Samples were analysed using a confocal laser-scanning microscope (LSM 700; Zeiss) with a 60" objective. Digital optical sections were obtained by scanning the samples on the z-axis at 0.29 μm thickness throughout the whole spindle. The z-series were then projected to obtain a three-dimensional image. Instrument settings for the red and blue channels (acH4K16 and DNA, respectively) were kept constant.
Image analysis was carried out using NIH ImageJ 1.4 Software. The spindle diameter and length were measured three times for each sample and the mean of the three measurements was considered for further analysis. The quantification of the relative fluorescence of acH4K16 was measured on digitised images and normalised to DAPI staining, representing total DNA.

RNA purification, reverse transcription and polymerase chain reaction
After cumulus cells removal, the oocytes were washed in PBS– PVA and collected singly in 1 mL at the bottom of a microtube. The granulosa cells from two to five 5–25-mm follicles were pooled and washed twice in cold PBS by centrifuging at 10 600g for 2 min at room temperature. The samples were covered with 2 mL RNA Later (Ambion, Huntingdon, UK) and snap frozen at the end of each collection session. For the RNA extraction the oocytes were pooled two by two in the extraction buffer of the PicoPure RNA Isolation Kit (Arcturus by Life Technologies, Saint Aubin, France) and 2 pg of Luciferase RNA (Promega, Charbonnieres-les-bains, France) were added as an external standard. Six or seven pools of oocytes for each experimental group (GV, in vivo matured and in vitro matured) were processed. Total DNase-treated RNA was extracted from oocytes and granulosa cells following the manufacturer's instructions.
The RNA was reverse transcribed in 10 mL with 0.25 mg random hexamers and mouse Moloney leukaemia virus reverse transcriptase (Invitrogen) for 1 h at 378C. Real-time PCR was performed on a MyiQ Cycler apparatus (Bio-Rad, Marnes-la- Coquette, France). Reactions were performed in a total volume of 20 mL using cDNA equivalent to 0.05 oocytes as substrate, SYBR green Bio-Rad supermix and 0.3 mM of each specific primer (Table 1). A three-step protocol (958C for 30 s, 608C for 30 s, 728C for 20 s) was repeated for 40 cycles, followed by acquisition of the melting curve. Serial dilutions of a known amount of cDNA, ranging from 50 to 0.01 ng, derived from the follicular granulosa cells, were used to calculate a standard curve and assess the starting quantity (SQ) of the specificmRNA in the oocyte samples, considering the median value of triplicate reactions. The expected amplicon sizes are shown in Table 1. The data are expressed as the ratio between the SQ of the gene of interest and the SQ of GAPDH, representing the housekeeping gene.

Table 1. List of primers

Target gene	Forward primer	Reverse primer	Amplicon size
GAPDH	ATCACCATCTTCCAGGAGCGAGA	GTCTTCTGGGTGGCAGTGATGG	241 bp
HAT1	CTGACATGAGTGATGCTGAACA	TAACGCGTCGGTAATCTTCC	219 bp
HDAC1	GAAGGCGGTCGCAAGAAT	CCAACTTGACCTCCTCCTTGA	166 bp
KAT8	ACTGGTCTTGGGTCCTGCTG	GGGCACTTTTGAGGTGTTCC	198 bp
Luciferase	TCATTCTTCGCCAAAAGCACTCTG	AGCCCATATCCTTGTCGTATCCC	148 bp
SIRT1	GACTCGCAAAGGAGCAGATT	GGACTCTGGCATGTTCCACT	169 bp

Statistical analysis

The aneuploidy rate between in vitro- and in vivo-matured oocytes was compared by Fisher's exact test. Data on the spindle diameter, spindle length and the relative fluorescence of acH4K16 were analysed by unpaired t-test. The Pearson coefficient (r) was calculated to express the correlation between acH4K16 and spindle length, and between acH4K16 and spindle diameter. Real-time PCR data were analysed by one-way ANOVA. P values < 0.05 were considered to be statistically significant. Results are presented as mean ± s.e.m. unless otherwise specified.

Results

The incidence of aneuploidy is increased in in vitro-matured oocytes

In order to study whether IVM can perturb the chromosome–spindle interaction during the first meiotic division, the number of chromosomes at the MII stage was counted, as it represents the result of chromosome segregation during meiosis I. Antibodies anti-CENPA (ab13939; Abcam, Cambridge, UK) and anti-AURKB (ab3609; Abcam) failed to localise to the centromeres in MII-stage horse oocytes (data not shown). In our hands, the anti-Aurora B phospho-Thr232 antibody was considered a good marker for the centromeric region in horse oocytes (Fig. 1a).

In vitro-matured oocytes had a significantly higher percentage of aneuploidy (5/11) when compared with in vivo-matured oocytes (0/12; Fisher's exact test, $P<0.05$; Fig. 1b). Specifically, 4/5 of the aneuploid in vitro-matured oocytes were hyperploid, with a chromosomal count >32, while one oocyte was hypoploid, with a chromosomal count of 28. Examples of euploid and aneuploid chromosomal counts carried out on sequential confocal sessions are given in Fig. S1, available as Supplementary Material to this paper.

Spindle anomalies are increased in in vitro-matured oocytes and correlate with H4K16 deacetylation

Representative images of bipolar (normal) and irregular spindles are given in Fig. 2 (also see Supplemental Movie for an example of a monopolar spindle). Fifty per cent of the in vitromatured oocytes showed evident morphological anomalies, like multipolar or monopolar spindles (4/14) and chromosomes scattered throughout the spindle structure (3/14), whereas all the in vivo-matured oocytes (4/4) showed bipolar spindles with chromosomes aligned on the metaphasic plate. The structure of the spindle looked more compact in in vivo-matured oocytes when compared with the in vitro-matured ones, which is

in agreement with a previous report in mice (Sanfins et al. 2003). In order to confirm this morphological observation, the diameter of the spindle was measured at the maximum width at the metaphasic plate level; the spindle length was considered to be the maximal distance between the two poles (Fig. 3a). These measurements demonstrated that in vitro-matured oocytes have a significantly larger diameter (17.28±0.81 μm) and pole-to-pole distance (19.89±1.15 μm) compared with in vivo-matured oocytes (13.56±0.91 mmdiameter and 14.57±1.7 μm length; unpaired t-test, $P<0.05$). Even though not statistically significant ($P=0.1286$), the acetylation level of H4K16 was negatively correlated with the length of the spindle ($r=-0.42$; Fig. 3b). No correlation was observed between H4K16 acetylation and spindle diameter ($r=-0.12$; Fig. 3c, $P=0.5902$).
Overall, the global acetylation at H4K16 was significantly lower in IVM oocytes compared with their in vivo counterparts (Fig. 3a and Fig. S2), confirming our previous results.

Expression of transcripts encoding for histone acetyltransferases (HATs) and deacetylases (HDACs) during horse oocyte maturation
We investigated whether differences in histone H4 acetylation between in vitro- and in vivo-matured oocytes were associated with altered expression of four genes involved in this process: two HATs (HAT1 and KAT8) and two HDACs (HDAC1 and SIRT1). Relative mRNA expression was assessed by real-time PCR in seven pools of GV-stage, seven pools of in vivo matured and six pools of in vitro-matured oocytes (Fig. 4). We did not observe any significant difference in the expression of HAT1, KAT8, HDAC1 or SIRT1 between the three classes of oocytes, independent of the meiotic stage or the maturation conditions. Similar results were obtained by normalising the mRNA relative abundance against the spike-in mRNA Luciferase (Fig. S3).

Discussion

Oocyte in vitro maturation (IVM) represents a less drugoriented, less expensive and more patient-friendly approach in assisted reproductive technology (ART) compared with ovarian hormonal stimulation. However, the use of IVM in human infertility treatment is still limited because it can increase the incidence of aneuploidy (Nogueira et al. 2000; Emery et al. 2005; Requena et al. 2009) with consequent risk of embryo–fetal loss and genetic diseases. A deeper knowledge of the molecular basis of chromosomal mis-segregation during IVM will increase the possibilities of developing safer IVM procedures. Here we propose the use of a monovulatory animal model, the mare, to investigate the process of oocyte maturation and to compare in vivo and in vitro conditions.
We first tested whether the occurrence of errors in chromosome segregation was increased in in vitro-matured horse oocytes, as happens in humans (Nogueira et al. 2000; Emery et al. 2005). A previous study, where the ploidy of horse embryos was investigated by fluorescent in situ hybridization (FISH), indicates that the nuclei of in vitro-produced embryos are more likely to be affected by chromosomal abnormalities than in vivo-produced embryos (Rambags et al. 2005). However, despite the fact that IVM has been performed in horses for more than 20 years (Choi et al. 1993; Hinrichs et al. 1993), whether the oocyte can be the origin of embryonic aneuploidy has never been tested. The

reason can partially reside in the fact that the preparation of oocyte spreads for chromosome counting usually results in considerable sample loss. With this in mind, we adapted a technique recently described in mouse oocytes (Duncan et al. 2009; Chiang et al. 2010) where the kinesin-5 inhibitor monastrol was used to collapse the spindle and disperse the chromosomes. This treatment allowed us to count the chromosomes without preparation of chromosomal spreads.

We observed that in vitro-matured oocytes are significantly more prone to undergo defects in chromosome segregation during meiosis I compared with their in vivo counterparts. These results demonstrate that aneuploidies in horses can originate in the oocyte during meiosis I, similar to what has been described in humans (Hassold and Hunt 2001). Notably, the incidence of aneuploidy that we observed in IVM oocytes was higher than the one reported for in vitro-produced embryos (Rambags et al. 2005), possibly suggesting that severe aneuploidies are not compatible with early embryonic development. Overall our results indicate that horse oocytes could be a valid cellular model for studying human aneuploidy during IVM compared with mouse oocytes, which are only minimally affected by aneuploidy.

In a second set of experiments we analysed the morphology of the meiotic spindle in in vivo- and in vitro-matured oocytes. Some spindle anomalies, such as monopolar or multipolar spindles or chromosomes scattered throughout the spindle rather than aligned at the spindle equator, were observed in in vitromatured oocytes, in agreement with previous studies (Goudet et al. 1997). In vivo-matured oocytes instead consistently showed a compact structure and bipolar morphology. Further morphometric analysis also demonstrated that bipolar, apparently normal, IVM spindles are significantly longer and wider compared with in vivo ones. Our observations on horse oocytes support the hypothesis that aneuploidies can arise from defective spindle formation during IVM, as already proposed by Sanfins et al. (2003), i.e. that altering the proper tension of microtubules can interfere with normal chromosome segregation.

In a recent study we observed that IVM also affects the acetylation pattern of H4K16, while residues K8 and K12 were not altered (Franciosi et al. 2012). Specifically H4K16 is acetylated at the GV stage. Upon maturation H4K16 remains acetylated in in vivo-matured oocytes, while it undergoes deacetylation following IVM.

In somatic cells, H4K16 deacetylation is generally thought to be necessary for chromatin condensation and silencing of gene expression (Shogren-Knaak et al. 2006). However, other studies have demonstrated that acetylated H4K16 can be found in association with repressor proteins (Robin et al. 2007) and whether acetylated H4K16 inhibits or promotes the chromatin remodelling complex ATPase Imitation of SWI (ISWI), is still a matter of debate (Klinker et al. 2014).

In the case of the transcriptionally inactive MII-stage oocytes, the global H4K16 acetylation can hardly be related to active gene expression, while a role in chromatin condensation seems more likely. We hypothesise that acetylated H4K16 promotes the recruitment of factors necessary for proper chromosome aggregation and for the interactions with proteins of the meiotic apparatus. This hypothesis is partially supported by the observation that one of the spindle anomalies found in IVM horse oocytes correlates with the deacetylation of H4K16, but this still requires extensive testing.

Studies conducted in a mouse model null for histone deacetylase 2 (Hdac2$^{-/-}$) showed that the hyperacetylation of H4K16 is associated with weakened kinetochore–microtubule attachment and increased chromosome segregation errors (Ma and Schultz 2013). These results are only apparently in conflict with our hypothesis. In fact, they demonstrate that perturbing the acetylation pattern of H4K16 leads to aneuploidies and alters chromosome–spindle interactions. Importantly, both studies agree that a normal acetylation state (in vivo-matured horse oocytes and wild-type mice) is associated with proper chromosome segregation and normal spindle assembly.

During oocyte maturation chromatin is transcriptionally inactive and the control of gene expression is exerted at the cytoplasmic level through the regulation of translation, storage and degradation of specific transcripts (Chen et al. 2011; Ma et al. 2013). In this view we reasoned that IVM could interfere with such regulatory mechanisms, for instance by promoting the degradation of mRNAs involved in histone acetylation or by inhibiting the degradation of deacetylase transcripts. To test this hypothesis we investigated the relative mRNA abundance of four transcripts, two encoding for HATs and two encoding for HDACs. For each class we analysed one enzyme known to have a broad activity on different H4 K-residues (HAT1 and HDAC1, for the acetyltransferases and deacetylases, respectively; Parthun 2007; Ma and Schultz 2008) and one more specific to K16 (KAT8-MYST1 and SIRT1 for the acetyltransferases and deacetylases, respectively; Peng et al. 2012; Marmorstein and Zhou 2014). We did not observe significant differences between in vivo and in vitro maturation in the expression of any of the genes considered. Our results demonstrate that impaired stability or degradation of HAT1, KAT8, HDAC1 and SIRT1 transcripts is not the mechanism responsible for the alteration of the pattern of histone acetylation during IVM. Even though we cannot exclude the involvement of other HATs or HDACs, it is more likely that control is achieved by regulating the amount or the enzymatic activity of HAT and HDAC proteins through posttranscriptional or post-translational mechanisms.

Finally, the relative mRNA abundance in MII oocytes (either in vivo- or in vitro-matured) was not significantly different from the GV stage, showing that these transcripts do not undergo degradation during meiosis I in horse oocytes. Similar profiles for HDAC1 and HAT1 mRNAs have been previously observed in bovine oocytes (McGraw et al. 2003). On the other hand, two studies described a decrease in HDAC1 mRNA during IVM in human oocytes (Wang et al. 2010; Huang et al. 2012). To the best of our knowledge, in these studies a mix of oligo-dT and random primers was used for reverse transcription, possibly introducing a bias for polyadenylated mRNAspecies rather than detecting a difference in the total mRNA abundance.

In the horse, IVM is applied to oocytes retrieved from antral follicles between 5 and 25mm(10–25mmin some laboratories). Larger follicles are not frequent and usually have a poor retrieval rate, therefore they cannot be consistently used. For this technical limitation we could not investigate whether IVM would equally affect GV oocytes collected from follicles >33 mm. In this vein, to the best of our knowledge, the diameter of the follicle of origin should be considered as one of the conditions inherent to IVM that, together with the other retrieval and culture procedures, might have contributed to the increased aneuploidy rate and altered epigenetic marks observed in our study.

To conclude, in the present study we characterised the phenotype and started to investigate the molecular events related to IVM in an adult, naturally cycling, monovulatory species. This study also suggests that epigenetic instabilities triggered by IVM procedures may affect oocyte genetic stability.

Acknowledgements
The authors would like to thank Fabrice Vincent for support with laser scanning confocal microscopy (LSCM) and Guy Duchamp for collaborating with the collection of oocytes from the mares. This work was supported in part by 'Regione Sardegna and Regione Lombardia', project 'Ex Ovo Omnia' (Grant no. 26096200 to A. M. L.), by 'L'Oreal Italia per le Donne e la Scienza 2012' fellowship (Contract 2012 to F. F.), by FP7-PEOPLE-2011- CIG, Research Executive Agency (REA) 'Pro-Ovum' (Grant no. 303640 to V. L.) and by the Postdoctoral School of Agriculture and Veterinary Medicine, co-financed by the European Social Fund, Sectorial Operational Program for Human Resource Development 2007–2013 (Contract no. POSDRU/89/1.5/S/62371 to I. M.). The in vivo oocyte collection was financed by the Institut Franc¸ais du Cheval et de l'Equitation.

References
Akiyama, T., Nagata, M., and Aoki, F. (2006). Inadequate histone deacetylation during oocyte meiosis causes aneuploidy and embryo death in mice. Proc. Natl. Acad. Sci. USA 103, 7339–7344. doi:10.1073/PNAS. 0510946103
Bartmann, A. K., Romao, G. S., Ramos Eda, S., and Ferriani, R. A. (2004). Why do older women have poor implantation rates? A possible role of the mitochondria. J. Assist. Reprod. Genet. 21, 79–83. doi:10.1023/ B:JARG.0000027018.02425.15
Campos-Chillon, F., Farmerie, T. A., Bouma, G. J., Clay, C. M., and Carnevale, E. M. (2015). Effects of aging on gene expression and mitochondrial DNA in the equine oocyte and follicle cells. Reprod. Fertil. Dev. doi:10.1071/RD14472
Carnevale, E. M. (2008). The mare model for follicular maturation and reproductive ageing in the woman. Theriogenology 69, 23–30. doi:10.1016/J.THERIOGENOLOGY.2007.09.011
Chen, J., Melton, C., Suh, N., Oh, J. S., Horner, K., Xie, F., Sette, C., Blelloch, R., and Conti, M. (2011). Genome-wide analysis of translation reveals a critical role for deleted in azoospermia-like (Dazl) at the oocyte-to-zygote transition. Genes Dev. 25, 755–766. doi:10.1101/ GAD.2028911
Cheng, E. Y., Hunt, P. A., Naluai-Cecchini, T. A., Fligner, C. L., Fujimoto, V. Y., Pasternack, T. L., Schwartz, J. M., Steinauer, J. E., Woodruff, T. J., Cherry, S. M., Hansen, T. A., Vallente, R. U., Broman, K. W., and Hassold, T. J. (2009). Meiotic recombination in human oocytes. PLoS Genet. 5, e1000661. doi:10.1371/JOURNAL.PGEN.1000661
Chiang, T., Duncan, F. E., Schindler, K., Schultz, R. M., and Lampson, M. A. (2010). Evidence that weakened centromere cohesion is a leading cause of age-related aneuploidy in oocytes. Curr. Biol. 20, 1522–1528. doi:10.1016/J.CUB.2010.06.069
Choi, Y. H., Hochi, S., Braun, J., Sato, K., and Oguri, N. (1993). In vitro maturation of equine oocytes collected by follicle aspiration and by the slicing of ovaries. Theriogenology 40, 959–966. doi:10.1016/0093- 691X(93)90364-B

Clayton, A. L., Hazzalin, C. A., and Mahadevan, L. C. (2006). Enhanced histone acetylation and transcription: a dynamic perspective. Mol. Cell 23, 289–296. doi:10.1016/J.MOLCEL.2006.06.017
Cox, L., Vanderwall, D. K., Parkinson, K. C., Sweat, A., and Isom, S. C. (2015). Expression profiles of select genes in cumulus–oocyte complexes from young and aged mares. Reprod. Fertil. Dev. doi:10.1071/RD14446
Donadeu, F. X., and Pedersen, H. G. (2008). Follicle development in mares. Reprod. Domest. Anim. 43(Suppl 2), 224–231. doi:10.1111/J.1439-0531.2008.01166.X
Duncan, F. E., Chiang, T., Schultz, R. M., and Lampson, M. A. (2009). Evidence that a defective spindle assembly checkpoint is not the primary cause of maternal age-associated aneuploidy in mouse eggs. Biol. Reprod. 81, 768–776. doi:10.1095/BIOLREPROD.109. 077909
Eichenlaub-Ritter, U. (2012). Oocyte ageing and its cellular basis. Int. J. Dev. Biol. 56, 841–852. doi:10.1387/IJDB.120141UE
Eichenlaub-Ritter, U., Vogt, E., Yin, H., and Gosden, R. (2004). Spindles, mitochondria and redox potential in ageing oocytes. Reprod. Biomed Online 8, 45–58. doi:10.1016/S1472-6483(10)60497-X
Emery, B. R., Wilcox, A. L., Aoki, V. W., Peterson, C. M., and Carrell, D. T. (2005). In vitro oocyte maturation and subsequent delayed fertilisation is associated with increased embryo aneuploidy. Fertil. Steril. 84, 1027–1029. doi:10.1016/J.FERTNSTERT.2005.04.036
Franciosi, F., Lodde, V., Goudet, G., Duchamp, G., Deleuze, S., Douet, C., Tessaro, I., and Luciano, A. M. (2012). Changes in histone H4 acetylation during in vivo versus in vitro maturation of equine oocytes. Mol. Hum. Reprod. 18, 243–252. doi:10.1093/MOLEHR/GAR077
Ginther, O. J. (2012). The mare: a 1000-pound guinea pig for study of the ovulatory follicular wave in women. Theriogenology 77, 818–828. doi:10.1016/J.THERIOGENOLOGY.2011.09.025
Ginther, O. J., Gastal, E. L., Gastal, M. O., Bergfelt, D. R., Baerwald, A. R., and Pierson, R. A. (2004). Comparative study of the dynamics of follicular waves in mares and women. Biol. Reprod. 71, 1195–1201. doi:10.1095/BIOLREPROD.104.031054
Goudet, G., Bezard, J., Duchamp, G., Gerard, N., and Palmer, E. (1997). Equine oocyte competence for nuclear and cytoplasmic in vitro maturation: effect of follicle size and hormonal environment. Biol. Reprod. 57, 232–245. doi:10.1095/BIOLREPROD57.2.232
Hassold, T., and Hunt, P. (2001). To err (meiotically) is human: the genesis of human aneuploidy. Nat. Rev. Genet. 2, 280–291. doi:10.1038/35066065
Hendriks, W. K., Colleoni, S., Galli, C., Paris, D. B., Colenbrander, B., Roelen, B. A., and Stout, T. A. (2015). Maternal age and in vitro culture affect mitochondrial number and function in equine oocytes and embryos. Reprod. Fertil. Dev. doi:10.1071/RD14450
Hinrichs, K., Schmidt, A. L., Friedman, P. P., Selgrath, J. P., and Martin, M. G. (1993). In vitro maturation of horse oocytes: characterisation of chromatin configuration using fluorescence microscopy. Biol. Reprod. 48, 363–370. doi:10.1095/BIOLREPROD48.2.363
Homer, H. A., McDougall, A., Levasseur, M., Yallop, K., Murdoch, A. P., and Herbert, M. (2005). Mad2 prevents aneuploidy and premature proteolysis of cyclin B and

securin during meiosis I in mouse oocytes. Genes Dev. 19, 202–207. doi:10.1101/GAD.328105
Huang, J., Li, T., Ding, C. H., Brosens, J., Zhou, C. Q., Wang, H. H., and Xu, Y. W. (2012). Insufficient histone-3 lysine-9 deacetylation in human oocytes matured in vitro is associated with aberrant meiosis. Fertil. Steril. 97, 178–184e3. doi:10.1016/J.FERTNSTERT.2011.10.023
Jones, K. T., and Lane, S. I. (2013). Molecular causes of aneuploidy in mammalian eggs. Development 140, 3719–3730. doi:10.1242/DEV. 090589
Klinker, H., Mueller-Planitz, F., Yang, R., Forne, I., Liu, C. F., Nordenskiold, L., and Becker, P. B. (2014). ISWI remodelling of physiological chromatin fibres acetylated at lysine 16 of histone H4. PLoS One 9, e88411. doi:10.1371/JOURNAL.PONE.0088411
Li, X. C., Bolcun-Filas, E., and Schimenti, J. C. (2011). Genetic evidence that synaptonemal complex axial elements govern recombination pathway choice in mice. Genetics 189, 71–82. doi:10.1534/GENETICS.111.130674
Lombardi, P. M., Cole, K. E., Dowling, D. P., and Christianson, D. W. (2011). Structure, mechanism and inhibition of histone deacetylases and related metalloenzymes. Curr. Opin. Struct. Biol. 21, 735–743. doi:10.1016/J.SBI.2011.08.004
Luciano, A. M., Goudet, G., Perazzoli, F., Lahuec, C., and Gerard, N. (2006). Glutathione content and glutathione peroxidase expression in in vivo and in vitro-matured equine oocytes. Mol. Reprod. Dev. 73, 658–666. doi:10.1002/MRD.20469
Luo, Y. B., Ma, J. Y., Zhang, Q. H., Lin, F., Wang, Z. W., Huang, L., Schatten, H., and Sun, Q. Y. (2013). MBTD1 is associated with Pr-Set7 to stabilise H4K20me1 in mouse oocyte meiotic maturation. Cell Cycle 12, 1142–1150. doi:10.4161/CC.24216
Luzzo, K. M., Wang, Q., Purcell, S. H., Chi, M., Jimenez, P. T., Grindler, N., Schedl, T., and Moley, K. H. (2012). High-fat diet-induced developmental defects in the mouse: oocyte meiotic aneuploidy and fetal growth retardation/brain defects. PLoS One 7, e49217. doi:10.1371/JOURNAL. PONE.0049217
Ma, P., and Schultz, R. M. (2008). Histone deacetylase 1 (HDAC1) regulates histone acetylation, development and gene expression in preimplantation mouse embryos. Dev. Biol. 319, 110–120. doi:10.1016/J.YDBIO. 2008.04.011
Ma, P., and Schultz, R. M. (2013). Histone deacetylase 2 (HDAC2) regulates chromosome segregation and kinetochore function via H4K16 deacetylation during oocyte maturation in mouse. PLoS Genet. 9, e1003377. doi:10.1371/JOURNAL.PGEN.1003377
Ma, J., Flemr, M., Strnad, H., Svoboda, P., and Schultz, R. M. (2013). Maternally recruited DCP1A and DCP2 contribute to messenger RNA degradation during oocyte maturation and genome activation in mouse. Biol. Reprod. 88, 11. doi:10.1095/BIOLREPROD.112.105312
Marmorstein, R., and Zhou, M. M. (2014). Writers and readers of histone acetylation: structure, mechanism and inhibition. Cold Spring Harb. Perspect. Biol. 6, a018762. doi:10.1101/CSHPERSPECT.A018762
McGraw, S., Robert, C., Massicotte, L., and Sirard, M. A. (2003). Quantification of histone acetyltransferase and histone deacetylase transcripts during early bovine embryo development. Biol. Reprod. 68, 383–389. doi:10.1095/BIOLREPROD.102.005991

Nabti, I., Marangos, P., Bormann, J., Kudo, N. R., and Carroll, J. (2014). Dual-mode regulation of the APC/C by CDK1 and MAPK controls meiosis I progression and fidelity. J. Cell Biol. 204, 891–900. doi:10.1083/JCB.201305049
Nichols, S. M., Gierbolini, L., Gonzalez-Martinez, J. A., and Bavister, B. D. (2010). Effects of in vitro maturation and age on oocyte quality in the rhesus macaque Macaca mulatta. Fertil. Steril. 93, 1591–1600. doi:10.1016/J.FERTNSTERT.2008.12.141
Nogueira, D., Staessen, C., Van de Velde, H., and Van Steirteghem, A. (2000). Nuclear status and cytogenetics of embryos derived from in vitro-matured oocytes. Fertil. Steril. 74, 295–298. doi:10.1016/ S0015-0282(00)00642-7
Parthun, M. R. (2007). Hat1: the emerging cellular roles of a type B histone acetyltransferase. Oncogene 26, 5319–5328. doi:10.1038/SJ.ONC. 1210602
Peng, L., Ling, H., Yuan, Z., Fang, B., Bloom, G., Fukasawa, K., Koomen, J., Chen, J., Lane, W. S., and Seto, E. (2012). SIRT1 negatively regulates the activities, functions and protein levels of hMOF and TIP60. Mol. Cell. Biol. 32, 2823–2836. doi:10.1128/MCB.00496-12
Rambags, B. P., Krijtenburg, P. J., Drie, H. F., Lazzari, G., Galli, C., Pearson, P. L., Colenbrander, B., and Stout, T. A. (2005). Numerical chromosomal abnormalities in equine embryos produced in vivo and in vitro. Mol. Reprod. Dev. 72, 77–87. doi:10.1002/MRD.20302
Rambags, B. P., van Boxtel, D. C., Tharasanit, T., Lenstra, J. A., Colenbrander, B., and Stout, T. A. (2014). Advancing maternal age predisposes to mitochondrial damage and loss during maturation of equine oocytes in vitro. Theriogenology 81, 959–965. doi:10.1016/J.THERIOGENOLOGY.2014.01.020
Requena, A., Bronet, F., Guillen, A., Agudo, D., Bou, C., and Garcia-Velasco, J. A. (2009). The impact of in vitro maturation of oocytes on aneuploidy rate. Reprod. Biomed. Online 18, 777–783. doi:10.1016/ S1472-6483(10)60026-0
Roberts, R., Iatropoulou, A., Ciantar, D., Stark, J., Becker, D. L., Franks, S., and Hardy, K. (2005). Follicle-stimulating hormone affects metaphase I chromosome alignment and increases aneuploidy in mouse oocytes matured in vitro. Biol. Reprod. 72, 107–118. doi:10.1095/BIOLREPROD.104.032003
Robin, P., Fritsch, L., Philipot, O., Svinarchuk, F., and Ait-Si-Ali, S. (2007). Post-translational modifications of histones H3 and H4 associated with the histone methyltransferases Suv39h1 and G9a. Genome Biol. 8, R270. doi:10.1186/GB-2007-8-12-R270
Ruggeri, E., DeLuca, K. F., Galli, C., Lazzari, G., DeLuca, J. G., and Carnevale, E. M. (2015). Cytoskeletal alterations associated with donor age and culture interval for equine oocytes and potential zygotes that failed to cleave after intracytoplasmic sperm injection. Reprod. Fertil. Dev. doi:10.1071/RD14468
Sanfins, A., Lee, G. Y., Plancha, C. E., Overstrom, E. W., and Albertini, D. F. (2003). Distinctions in meiotic spindle structure and assembly during in vitro and in vivo maturation of mouse oocytes. Biol. Reprod. 69, 2059–2067. doi:10.1095/BIOLREPROD.103.020537
Shin, Y. H., Choi, Y., Erdin, S. U., Yatsenko, S. A., Kloc, M., Yang, F., Wang, P. J., Meistrich, M. L., and Rajkovic, A. (2010). Hormad1 mutation disrupts synaptonemal complex formation, recombination and chromosome segregation in mammalian meiosis. PLoS Genet. 6, e1001190. doi:10.1371/JOURNAL.PGEN.1001190

Shogren-Knaak, M., Ishii, H., Sun, J. M., Pazin, M. J., Davie, J. R., and Peterson, C. L. (2006). Histone H4–K16 acetylation controls chromatin structure and protein interactions. Science 311, 844–847. doi:10.1126/ SCIENCE.1124000
Shomper, M., Lappa, C., and FitzHarris, G. (2014). Kinetochore microtubule establishment is defective in oocytes from aged mice. Cell Cycle 13, 1171–1179. doi:10.4161/CC.28046
te Velde, E. R., and Pearson, P. L. (2002). The variability of female reproductive ageing. Hum. Reprod. Update 8, 141–154. doi:10.1093/ HUMUPD/8.2.141
Tsutsumi, M., Fujiwara, R., Nishizawa, H., Ito, M., Kogo, H., Inagaki, H., Ohye, T., Kato, T., Fujii, T., and Kurahashi, H. (2014). Age-related decrease of meiotic cohesins in human oocytes. PLoS One 9, e96710. doi:10.1371/JOURNAL.PONE.0096710
Turner, B. M. (2014). Nucleosome signalling: an evolving concept. Biochim. Biophys. Acta 1839, 623–626. doi:10.1016/J.BBAGRM.2014.01.001
Wang, N., Le, F., Zhan, Q. T., Li, L., Dong, M. Y., Ding, G. L., Xu, C. M., Jiang, S. W., Huang, H. F., and Jin, F. (2010). Effects of in vitro maturation on histone acetylation in metaphase II oocytes and early cleavage embryos. Obstet. Gynecol. Int. 2010, 989278. doi:10.1155/2010/989278
Yang, F., Baumann, C., Viveiros, M. M., and De La Fuente, R. (2012). Histone hyperacetylation during meiosis interferes with large-scale chromatin remodelling, axial chromatid condensation and sister chromatid separation in the mammalian oocyte. Int. J. Dev. Biol. 56, 889–899. doi:10.1387/IJDB.120246RD
Yun, Y., Holt, J. E., Lane, S. I., McLaughlin, E. A., Merriman, J. A., and Jones, K. T. (2014). Reduced ability to recover from spindle disruption and loss of kinetochore spindle assembly checkpoint proteins in oocytes from aged mice. Cell Cycle 13, 1938–1947. doi:10.4161/CC.28897
Zentner, G. E., and Henikoff, S. (2014). Regulation of nucleosome dynamics by histone modifications. Nat. Struct. Mol. Biol. 20, 259–266. doi:10.1038/NSMB.2470

Figure legends

Fig. 1. Chromosome count in in vivo- and in vitro-matured oocytes. (a) Representative images showing aurora B phospho-Thr232 (red) and DNA (green) staining of a MII-stage horse oocyte treated with monastrol. The merge between the red and green staining has been used to count the chromosomes. An euploid oocyte (32 chromosomes) is shown. Scale bar 5 μm. (b) The bar graph represents the distribution of euploid and aneuploid MII-stage oocytes in in vivo- (n=12) and in vitro- (n=11) matured oocytes. *Indicates significant difference in the aneuploidy rate (Fisher's exact test, $P<0.05$).

Fig. 2. Spindle morphology in in vivo- and in vitro-matured oocytes. Representative imagesshowing tubulin (green) and DNA (blue) staining in MII-stage horse oocytes after in vivo(n=4) or in vitro (n=14) maturation. Examples of bipolar, multipolar and monopolar spindlesand of chromosomes scattered throughout the spindle are given. Scale bar=5 μm.

Fig. 3. Measurement of spindle length and diameter and correlation with H4K16 acetylation. (a) Representative images showing tubulin (green), acetylated

H4K16 (red) and DNA (blue) in MII oocytes after in vivo (n=4) or in vitro maturation (n=14). The tubulin images show the axes used for spindle length and diameter measurements. Scale bar=5 μm. (b) The bar graph represents the measurement (mean±s.e.m.) of the spindle length in MII-stage oocytes after in vivo (n=4) or in vitro (n=14) maturation. The line graph represents the correlation between spindle length and acetylation at H4K16 (r=-0.42). (c) The bar graph represents the measurement (mean ± s.e.m.) of the spindle diameter in MII-stage oocytes after in vivo (n=4) or in vitro (n=14) maturation. The line graph represents the correlation between spindle diameter and acetylation at H4K16 (r=-0.12). *Indicates significant difference between in vivo and in vitro maturation (unpaired t-test, $P<0.05$).

Fig. 4. Expression of KAT8, SIRT1, HAT1 and HDAC1 in GV-stage, in vivo- and in vitromatured oocytes. The bar graphs represent the relative mRNA expression of KAT8, SIRT1, HAT1 and HDAC1 expressed as the starting quantity (SQ) of the gene of interest compared with the SQ of GAPDH, used as a housekeeping gene. No statistical differences were observed between GV (n=14), in vivo- (n=14) and in vitro- (n=12) matured oocytes (one-way ANOVA, $P<0.05$).

Fig.1

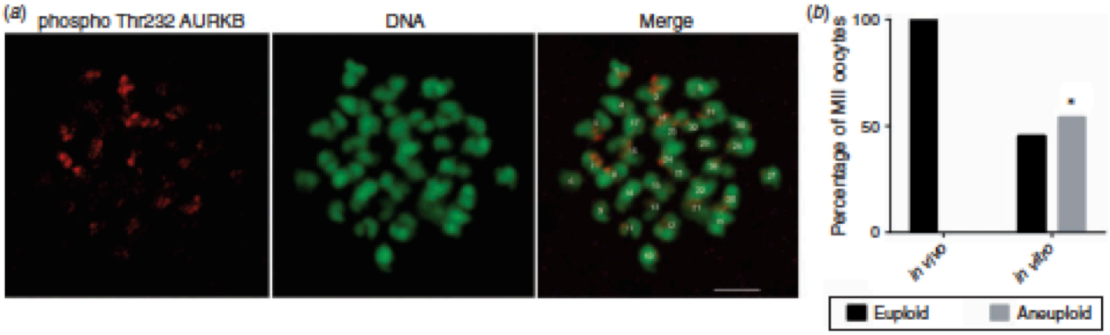
(a)
phospho Thr232 AURKB
DNA
Merge
(b)
Percentage of MII oocytes
100
50
0
*
in vivo
in vitro
Euploid
Aneuploid

Fig.2

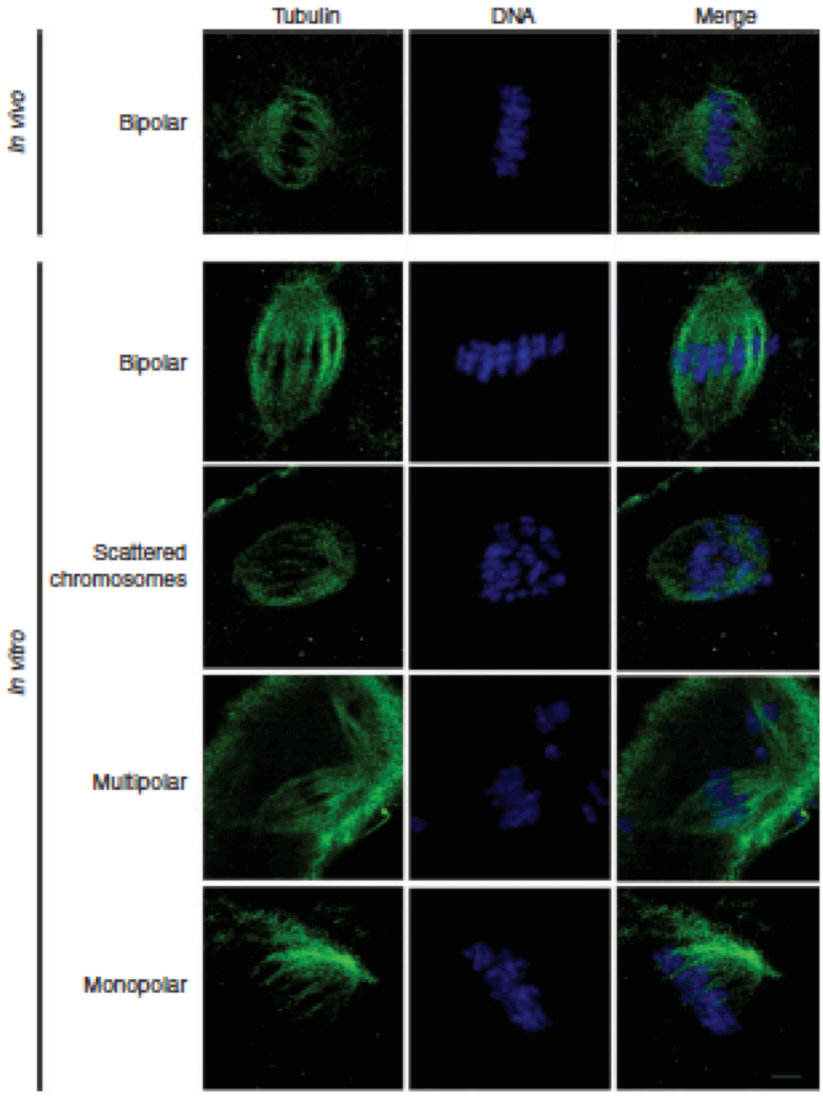
Tubulin
DNA
Merge
In vivo
Bipolar
In vitro
Bipolar
Scattered chromosomes
Multipolar
Monopolar

Fig.3

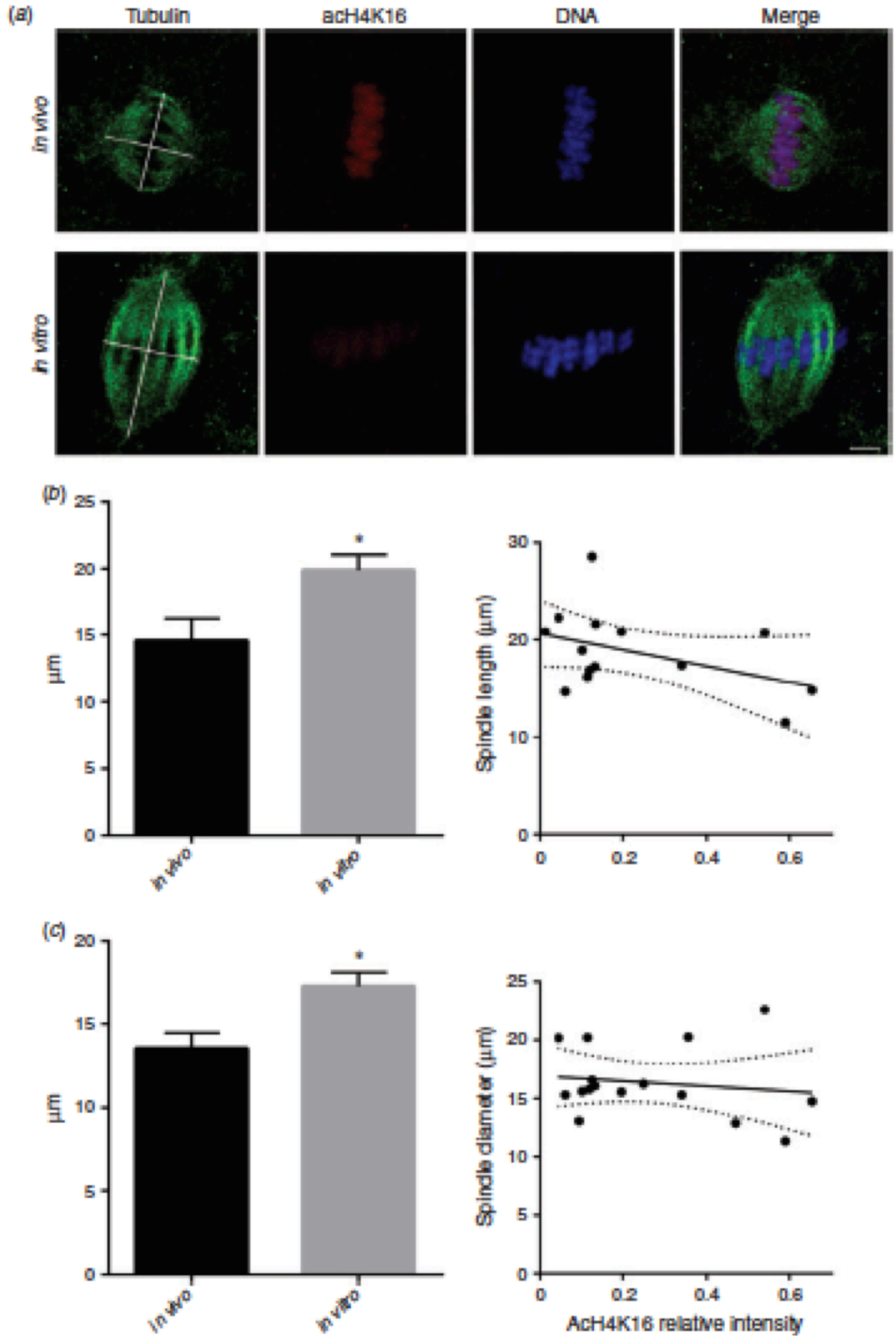
(a)
Tubulin
acH4K16
DNA
Merge
In vivo
In vitro
(b)
μm
In vivo
In vitro
Spindle length (μm)
(c)
μm
In vivo
In vitro
Spindle diameter (μm)
AcH4K16 relative intensity

Fig.4

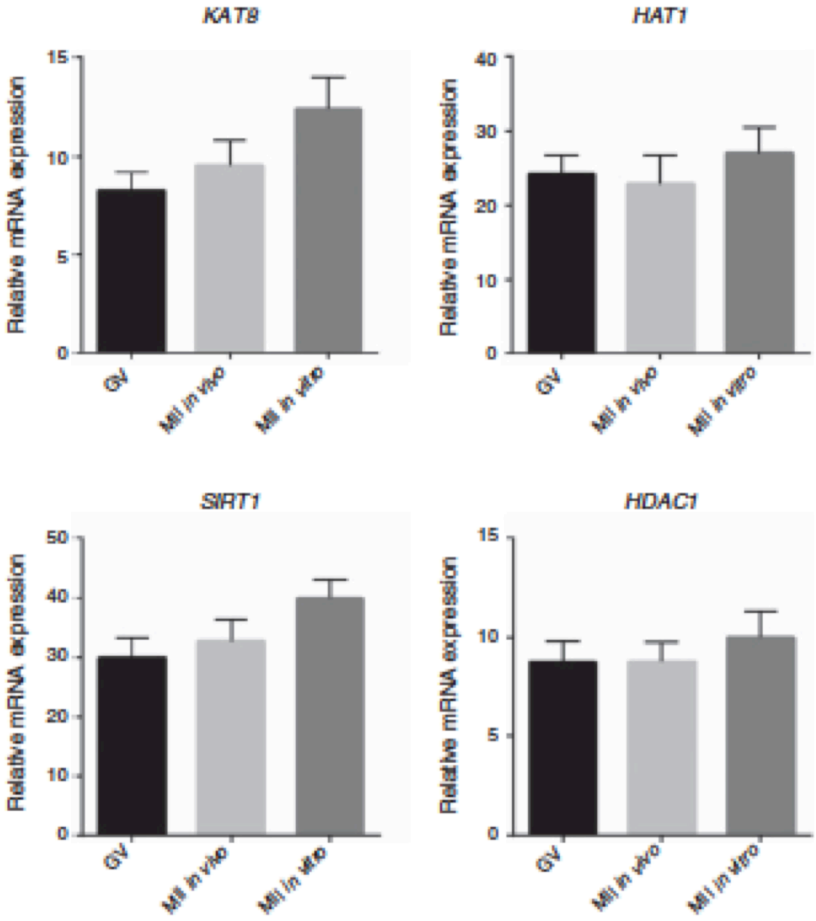
KAT8
HAT1
SIRT1
HDAC1
Relative mRNA expression
GV
MII in vivo
MII in vitro
0
5
10
15
20
30
40
50